




Topological Anderson insulating phases in the interacting Haldane model

João S. Silva ^{1,*} Eduardo V. Castro,^{2,†} Rubem Mondaini,^{3,‡} María A. H. Vozmediano ^{4,§} and M. Pilar López-Sancho ^{4,||}

¹*Centro de Física das Universidades do Minho e Porto, LaPMET, Departamento de Física e Astronomia, Faculdade de Ciências, Universidade do Porto, 4169-007 Porto, Portugal*

²*Centro de Física das Universidades do Minho e Porto, Departamento de Física e Astronomia, Faculdade de Ciências, Universidade do Porto, 4169-007 Porto, Portugal*

³*Beijing Computational Science Research Center, Beijing 100084, China*

⁴*Instituto de Ciencia de Materiales de Madrid, CSIC, Sor Juana Inés de la Cruz 3, Cantoblanco, 28049 Madrid, Spain*



(Received 7 September 2023; revised 12 March 2024; accepted 13 March 2024; published 26 March 2024)

We analyze the influence of disorder and strong correlations on the topology of two-dimensional Chern insulators. A mean-field calculation in the half-filled Haldane model with extended Hubbard interactions and Anderson disorder shows that the disorder favors topology in the interacting case and extends the topological phase to a larger region of the Hubbard parameters. In the absence of a staggered potential, we find a novel disorder-driven topological phase with Chern number $C = 1$, with the coexistence of topology with long-range spin and charge orders. More conventional topological Anderson insulating phases are also found in the presence of a finite staggered potential.

DOI: [10.1103/PhysRevB.109.125145](https://doi.org/10.1103/PhysRevB.109.125145)

I. INTRODUCTION

Topological phases of physical systems are one of the pillars of modern condensed matter [1]. The topological features of a material are established at the noninteracting level, and the fate of topology in strongly correlated systems is a relevant topic of current research in the field [2]. Disorder, always present in real materials, also plays a vital role in the phase diagram of correlated electrons. Although strong disorder would be detrimental to topology, eventually leading to trivial, Anderson localized phases in two-dimensional (2D) systems [3], disorder-induced topological phases (Anderson topological insulators) [4] are an exciting possibility proposed recently. In this work, we explore the interplay of topology, disorder, and interactions using the Haldane model at half filling [5] as a paradigm of topological Chern insulators in two dimensions. For that, we consider the extended Hubbard model with on-site and nearest-neighbor (NN) U and V interactions, respectively, subjected to Anderson disorder W and explore the ensuing mean-field phase diagram.

The Haldane model was originally set as a lattice model of spinless electrons on the honeycomb lattice with nearest-neighbor (t) and complex next-nearest-neighbor ($t_2 e^{i\phi}$) hopping energy scales, as schematically shown in Fig. 1(a). At half filling, a sufficiently large staggered potential Δ ($|\Delta/t_2| > 3\sqrt{3}$) leads to a topologically trivial phase, whereas the value of t_2/t (combined with its corresponding phase ϕ)

promotes the topological regime, as shown by the solid line in the phase diagram in Fig. 1(b). These phases are identified by the value of the Chern number, which counts the number and chirality of edge modes via the bulk-boundary correspondence once open boundary conditions are considered. In particular, with added disorder, these topological regions in the phase diagram are deformed, as indicated by the colored regions in Fig. 1(b), here for $W = 4t$ [6]. In the presence of an added spin degree of freedom, the corresponding topological phases have a Chern number $C = \pm 2$.

It is well known [7] and will be further detailed later that an on-site interaction U drives the system to a spin density wave (SDW), while the NN interaction V promotes a charge density wave (CDW) phase. Both are topologically trivial insulators with a finite local order parameter emerging for each order type. The phase diagram of the clean, interacting model in the mean-field approximation is shown in Fig. 2(a) (dashed lines). We primarily aim to generalize these results to include quenched, uncorrelated disorder. An initial expectation is that a critical value of disorder strength will generally drive the topological insulator to a trivial Anderson insulator. Still, as we will see in what follows, the ensuing phases in the presence of interactions can be manifestly richer than that.

This paper is organized as follows: In Sec. II we introduce the model and the methods we use to analyze its properties. Our main findings are presented in Sec. III A. We put these results in context by comparing them with previous works in Sec. III B. In Sec. IV A, we provide details on the nature of the new disorder-driven topological $C = 1$ phase and discuss the effect of the disorder on the original phase boundaries of the clean phase diagram. The disordered phases arising with a finite staggered potential are reviewed in Sec. IV B. Open

*jss.joaossilva@gmail.com

†evcastro@fc.up.pt

‡rmondaini@csrc.ac.cn

§mahvozmediano@gmail.com

||pilar@icmm.csic.es

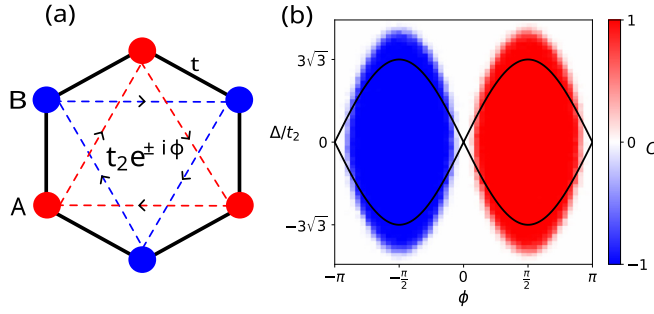


FIG. 1. (a) Schematic representation of the Haldane model on the honeycomb lattice with annotated terms for the hopping between nearest and next-nearest neighbors. (b) Phase diagram of the (non-interacting) spinless Haldane model as a function of the staggered potential and effective Haldane mass parametrized by the phase of the NNN hoppings. Here, the solid lines give the clean case ($W = 0$) result, whereas the colors map shows the topological regions in the presence of finite disorder ($W/t = 4$). We have set $t_2 = 0.2t$. The linear lattice size used in (b) is $L = 19$, and the Chern numbers are obtained by averaging over 100 disorder configurations. The Chern number is doubled in the spinful system.

questions and possible future works are discussed in Sec. V. Technical details on the model and calculations can be found in Appendix A.

II. MODEL AND METHODS

The Haldane model is described by the Hamiltonian [5]

$$H_0 = -t \sum_{\langle i,j \rangle} c_i^\dagger c_j - t_2 \sum_{\langle\langle i,j \rangle\rangle} e^{-i\phi_{ij}} c_i^\dagger c_j + \Delta \sum_i \eta_i c_i^\dagger c_i, \quad (1)$$

where $c_i = A, B$ are defined in the two triangular sublattices that form the honeycomb lattice. The first term t represents a standard real nearest-neighbor hopping that links the two

triangular sublattices. The t_2 term represents a complex next-nearest-neighbor (NNN) hopping $t_2 e^{-i\phi_{ij}}$ acting within each triangular sublattice with a phase ϕ_{ij} that has opposite signs $\phi_{ij} = \pm\phi$ (governing the chirality) in the two sublattices. The structure of the NNN hoppings is shown in Fig. 1(a). This term breaks time-reversal symmetry and opens a nontrivial topological gap at the Dirac points proportional to the magnitude of t_2 . We restrict the calculations to $\phi = \pi/2$ since it maximizes the topological region in the noninteracting regime [see the solid line in Fig. 1(b)] and take the value $t_2 = 0.2t$. The last term in Eq. (1) represents a staggered potential ($\eta_i = \pm 1$). It breaks inversion symmetry and opens a trivial gap at the Dirac points, as seen in Fig. 1(b). Spin doubles the degrees of freedom, and the Chern number is $C = \pm 2$ in the topological phases.

The interacting Hamiltonian we consider has the form

$$H_{\text{int}} = U \sum_i n_{i,\uparrow} n_{i,\downarrow} + V \sum_{\langle i,j \rangle, \sigma, \sigma'} n_{i,\sigma} n_{j,\sigma'}, \quad (2)$$

where $n_{i,\sigma} = c_{i,\sigma}^\dagger c_{i,\sigma}$ is the number operator. The on-site interaction term U penalizes double occupancy, thus favoring a homogeneous charge distribution between the two sublattices. In this sense, it goes against the staggered on-site potential Δ and can favor topology to some extent. U also has the effect of polarizing the spin, and over a critical value, it drives the system to a spin density wave insulator. The NN repulsive interaction V favors sublattice charge imbalance and, similar to Δ , goes against topology.

A chemical potential (Anderson) disorder is implemented by adding to the Hamiltonian the term $H_{\text{dis}} = \sum_{i \in A, B} \varepsilon_i c_i^\dagger c_i$, with a uniform distribution of random local energies, $\varepsilon_i \in [-W/2, W/2]$. This on-site term will contribute to the mean-field decoupling of the Hubbard U . Unless otherwise specified, the disorder averages were done using 50 disorder configurations.

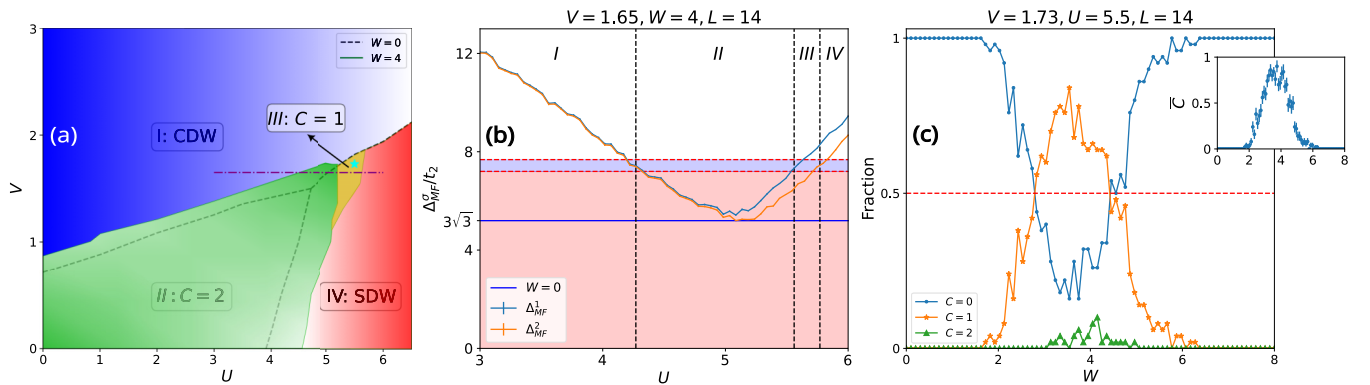


FIG. 2. (a) Phase diagram of the extended Haldane-Hubbard model on the half-filled honeycomb lattice as a function of the interactions U and V with zero staggered potential. The dashed lines mark the different phases in the absence of disorder. Solid lines separate the phases when Anderson disorder $W = 4$ is included. Four different phases are observed, including (I) a topologically trivial phase featuring charge order, (II) a topological Chern insulator with total Chern number $C = 2$, (III) a topologically nontrivial region but with $C = 1$, and (IV) a region exhibiting spin ordering that is topologically trivial. (b) Analysis of the effective staggered spin-dependent potential $\Delta_{\text{MF}}^\sigma$ [see Eq. (4)] along a line cut in (a) (see the horizontal dash-dotted line), with $V = 1.65$, which explains the spontaneous symmetry breaking of $SU(2)$ that leads to a $C = 1$ phase: the red-shaded region maps the topologically nontrivial region for this disorder strength in the noninteracting regime [see Fig. 1(b)]. (c) The fraction of disorder realizations that result in a given Chern number C for a specific point in the $C = 1$ phase [star in (a)] as a function of the disorder strength W ; the inset gives the corresponding average Chern number. The linear lattice size used in (b) and (c) is $L = 14$.

A mean-field decoupling of Eq. (2) gives

$$\begin{aligned}
 H_{\text{int}}^{\text{MF}} = & U \sum_{i,\sigma} [\langle n_{i,-\sigma} \rangle c_{i,\sigma}^\dagger c_{i,\sigma} - \langle c_{i,-\sigma}^\dagger c_{i,\sigma} \rangle c_{i,\sigma}^\dagger c_{i,-\sigma}] \\
 & + V \left[\sum_{\langle i,j \rangle, \sigma, \sigma'} \langle n_{j,\sigma'} \rangle c_{i,\sigma}^\dagger c_{i,\sigma} \right. \\
 & \left. - \sum_{(i,j), \sigma, \sigma'} \langle c_{j,\sigma'}^\dagger c_{i,\sigma} \rangle c_{i,\sigma}^\dagger c_{j,\sigma'} \right], \quad (3)
 \end{aligned}$$

where the fields $\langle c_{i,\sigma}^\dagger c_{j,\sigma'} \rangle$ are obtained self-consistently (see Appendix A). Finally, the total calculated Hamiltonian reads $H = H_0 + H_{\text{int}}^{\text{MF}} + H_{\text{dis}}$.

From the total calculated Hamiltonian H we define the effective staggered spin-dependent potential $\Delta_{\text{MF}}^\sigma$,

$$\Delta_{\text{MF}}^\sigma = \frac{1}{N} \sum_{i \in A} \frac{|\xi_{i,\sigma} - \xi_{j_i,\sigma}|}{2}, \quad (4)$$

where $j_i \in B$ is the NN of site i , which belongs to the same unit cell, and $\xi_{i,\sigma}$ is a diagonal element of H in the real-space tight-binding basis $c_i^\dagger |0\rangle = |i, \sigma\rangle$,

$$\langle i, \sigma | H | i, \sigma \rangle \equiv \xi_{i,\sigma} = U \langle n_{i,-\sigma} \rangle + V \sum_{\bar{\delta}, \sigma'} \langle n_{i+\bar{\delta}, \sigma'} \rangle + \varepsilon_i. \quad (5)$$

After disorder averaging, $\Delta_{\text{MF}}^\sigma$ turns out to be an important quantity for understanding the obtained results, as will be discussed in Sec. IV.

III. MAIN FINDINGS AND ANTECEDENTS

A. Main results

Figure 2 summarizes our main results. In particular, Fig. 2(a) shows the phase diagram of the disordered, spinful Haldane model as a function of the extended Hubbard interactions U and V in units of the NN hopping parameter t . The Haldane parameters are chosen in the topological region of Fig. 1(b) with zero staggered potential $\Delta = 0$ and $\phi = \pi/2$. The dashed lines mark the different phases in the absence of disorder for better comparison: the standard Chern insulator with Chern number $C = 2$ and the $C = 0$ SDW and CDW phases. Solid lines separate the phases when Anderson disorder $W = 4$ (in units of t) is included. The disorder is seen to enlarge the topological $C = 2$ region and to generate a novel $C = 1$ phase near the boundary of the three phases. This phase has long-range spin and charge orders. Figures 2(b) and 2(c) present an interpretation of this $C = 1$, which will be put forward in Sec. IV.

Finally, we highlight that the experimental realization of the Haldane model [8,9] and the ability to realize strongly correlated Hubbard models using cold-atom systems [10,11] give real prospects for emulating the spinful, extended Haldane-Hubbard model [12,13]. With the ability to include disorder [14,15], the door is open to direct confirmation of the results of this work.

B. Antecedents

The effect of disorder and/or Hubbard interactions on the Haldane model has a long history related to the nontopological honeycomb lattice. The phase diagram in Fig. 2 substituting the Chern insulator phase with a semimetal has been revisited over and over since the pioneering works in [16–19]. In this section we will discuss only the previous works that are closely related to our results.

(1) A $C = 1$ phase in the clean, spinful Haldane model with only on-site Hubbard U was found in [20–26] as an interplay of finite staggered potential Δ and U . No $C = 1$ was found in mean-field calculations with $\Delta = 0$. The new phase is spin polarized and was termed a “topological spin density wave.” An intuitive physical picture of this phase will be described in the next section. An important open question around this phase is whether or not it is an artifact of the used approximations, like the mean-field approximation, since it was not found in the dynamical cluster approximation in Ref. [27]. The $C = 1$ phase was recently reestablished with an exact diagonalization calculation in [26]. Its stability against long-range Coulomb interaction was examined in [25] using a diagrammatic Monte Carlo method.

(2) Topological transitions in the extended Haldane-Hubbard model (U, V) with zero staggered potential and no disorder ($\Delta = 0, W = 0$) were studied in [7]. No $C = 1$ phase was found there, except for a particular cluster used in the exact diagonalization attributed to finite-size effects. A variety of techniques led the authors to conclude that topological and locally ordered phases do not coexist in the model.

(3) Interestingly, a $C = 1$ phase was also found in the topological square lattice ($C = 2$ in the noninteracting limit) [23] with U and V interactions and a sublattice potential $\Delta = 2$. A mean-field calculation showed a $C = 1$ phase called the (interaction-driven) antiferromagnetic Chern insulator by the authors. As in previous works, this phase is not present when $\Delta = 0$.

(4) The interplay of NN interaction V , disorder, and topology in the spinless Haldane-Hubbard model was addressed in [28]. A topological Anderson insulator found in the noninteracting system with a finite staggered potential was shown to be stable to the presence of sufficiently small interactions.

The study of the effect of disorder in the spinful extended Haldane-Hubbard model is clearly missing. Also missing from previous results is a $C = 1$ phase with $\Delta = 0$.

IV. CHARACTERIZING THE NEW ANDERSON TOPOLOGICAL INSULATORS

A. Phase diagram in the $\Delta = 0$ case

The phase diagram of the $\Delta = 0$ case is shown in Fig. 2(a). The most interesting finding there is the $C = 1$ phase arising from the interplay of U, V , and W . It is a topological Anderson insulator phase that is highly disordered and shows a nonzero spin polarization and charge inhomogeneities (electron-hole puddles) with a nonzero mean value of the SDW and CDW order parameters. The spin and charge order parameters are defined in Eq. (A2). Their evolution as a function of the lattice size is shown in Fig. 3 (N is the number of unit cells). The circles are calculated points with the standard deviation of the mean shown as the error bars by the vertical lines (see

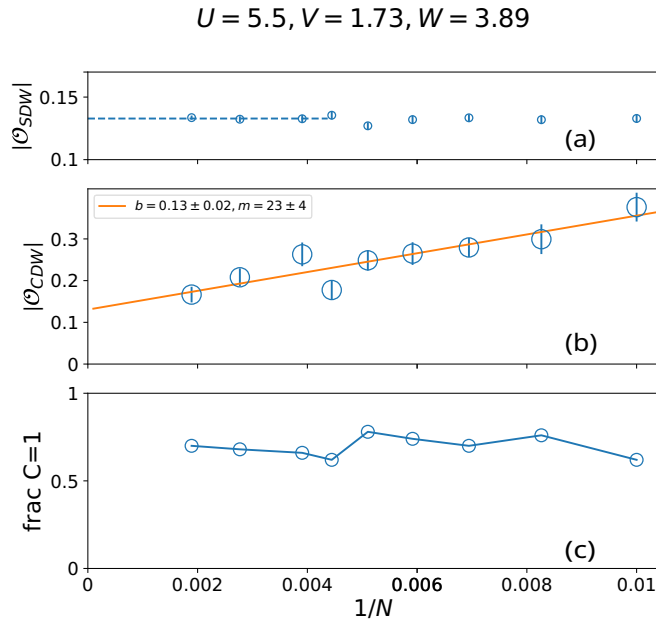


FIG. 3. (a) Spin and (b) charge order parameters in the $C = 1$ phase and (c) fraction of disorder configurations which yield $C = 1$ as a function of the inverse of lattice size $1/N$, with $N = L^2$ being the number of unit cells. The charge order parameter has been fitted to $|O_{CDW}| = m(1/N) + b$. The error bars are the standard error of the mean (see Appendix A).

Appendix A). As inferred from Fig. 3(a), it is clear that the spin order parameter will remain finite in the thermodynamic limit. The CDW order parameter shows more oscillations, but as is evident from the fit in Fig. 3(b) (see the caption), it does not extrapolate to zero. To illustrate the robustness of the $C = 1$ phase as the system size increases, we show in Fig. 3(c) the fraction of $C = 1$ disorder configurations as a function of $1/N$, where N is the number of unit cells. This result strongly indicates that the $C = 1$ phase is not a finite-size effect. A typical configuration of the charge inhomogeneity in the $C = 1$ phase is shown in Fig. 4 for $U = 5.5$, $V = 1.73$, and $W = 3.89$. This phase is at odds with the analysis in Ref. [7], which found no coexistence of topological and long-range-ordered phases in the clean model.

The $C = 1$ phase described previously in the spinful Haldane model [20–23,26,27,29,30] was due to the interplay of a staggered potential and the local Hubbard U interaction without NN interaction V in the clean topological lattice. The $C = 1$ phase was found in a narrow region between the two topologically trivial insulators induced by high values of the staggered potential (trivial insulator) and local U interaction (Mott-Hubbard insulator). The exotic phase was dubbed a topological spin density wave and is the same type as the one described here.

An intuitive understanding of the $C = 1$ phase works as follows: It is easy to see that, at the mean-field level, the CDW order parameter works like a staggered potential in the Haldane model, while the SDW order parameter works like a spin-dependent staggered potential, with opposite signs for the two spin polarizations. The presence of both SDW and CDW order parameters will act as a trivial gap for one spin polarization and reinforces the topological gap in the other.

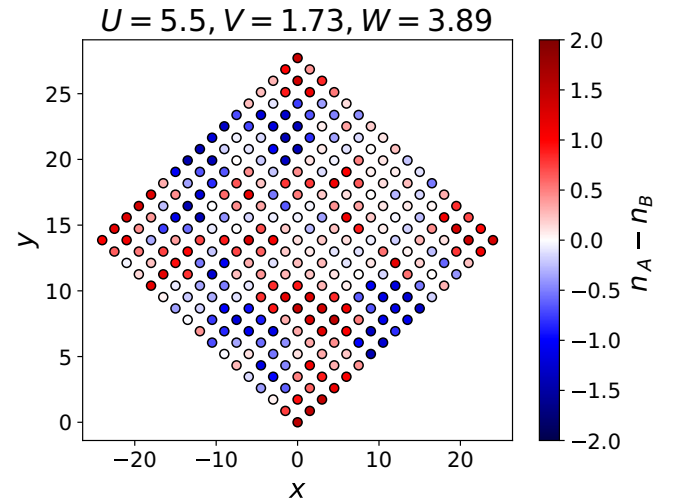


FIG. 4. Typical charge density imbalance in the $C = 1$ phase for a given disorder configuration. Each circle represents the difference between the electron densities of the two sublattices for a given unit cell ($n_A - n_B$), where $n_{\Gamma} = \sum_{\sigma=\uparrow,\downarrow} \langle n_{i \in \Gamma, \sigma} \rangle$. The linear lattice size used is $L = 17$.

As a consequence, with increasing U , the bands for one spin polarization will become trivial, while for the other they will still be topologically nontrivial. Since the Chern number is the sum of the two spin contributions, there will be a region in the parameter space where $C = 1$. This explanation of the $C = 1$ phase is sketched in Fig. 5. The left graph shows the bands of the Haldane model with zero staggered potential around the Dirac points K and K' . The bands are degenerated in spin and have an inverted gap. The CDW induced by a NN interaction V splits the degeneracy of the valleys as shown in the middle panel. The SDW due to an on-site interaction U lifts the spin degeneracy and moves the spin-polarized bands as indicated in the right panel. For a critical value of the parameters, the inverted gap closes in one of the spin-polarized bands that becomes topologically trivial, giving rise to the $C = 1$ phase. This explanation holds exactly for the $C = 1$ phase observed with $V = 0$ and finite staggered potential Δ . A finite Δ explicitly breaks sublattice symmetry and leads to a finite charge imbalance equivalent to CDW.

In comparison with previous works in the literature one is tempted to think that the role played by Δ there is taken by

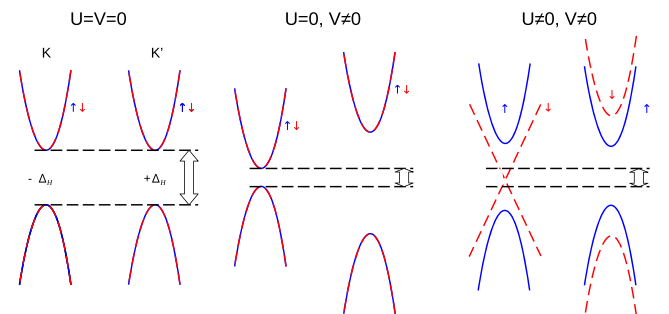


FIG. 5. Evolution of the Haldane bands around the K and K' points of the Brillouin zone under the effect of the interactions U and V . Δ_H is the topological gap of the Haldane model.

V in our case. However, the analysis of the clean extended Haldane-Hubbard model does not show the $C = 1$ phase [7]. In the clean limit, the simultaneous presence of CDW and SDW is energetically unfavorable. It is disorder that, allowing the coexistence of topological and long-range orders, permits the CDW order parameter to work as a trivial mass. This view is corroborated by Fig. 2(b), where we plot the effective staggered spin-dependent potential $\Delta_{\text{MF}}^{\sigma}$ given by Eq. (4) for fixed V and W and varying U along the horizontal dash-dotted line indicated in the phase diagram in Fig. 2(a). In the clean limit, this quantity plays the role of the effective gap for the spin-resolved bands shown in Fig. 5. The first horizontal line in Fig. 2(b) at $3\sqrt{3}t_2$ marks the topological transition in the clean, noninteracting Haldane model. In the presence of disorder, the topological region is wider [see Fig. 1(b) at $\phi = \pi/2$], as signaled by the red-shaded region in Fig. 2(b). The two horizontal dashed red lines locate, within the uncertainty due to disorder averaging, the topological transition for the disordered Haldane model. It is seen that, for small U , $\Delta_{\text{MF}}^{\sigma}$ is spin degenerate and has values above the topological transition. This agrees with the trivial CDW phase (region I) in the phase diagram in Fig. 2(a). Increasing U leads to a decrease in $\Delta_{\text{MF}}^{\sigma}$, which, for some critical interaction, falls below the topological transition line. This is compatible with the topological $C = 2$ phase (region II) in the phase diagram. With a further increase in U , the spin degeneracy of $\Delta_{\text{MF}}^{\sigma}$ is lifted, and the effective staggered potentials start to increase with U . At some point, one of the effective spin-dependent staggered potentials rises above the topological transition line, while the other is still below it. The system should then have $C = 1$, which is fully compatible with region III in the phase diagram. Astonishingly, the phase boundaries in Fig. 2(b) are almost in quantitative agreement with the true phase diagram in Fig. 2(a). This clearly indicates that, indeed, V plays the role of Δ in the present case, as long as disorder is high enough.

The key role played by disorder is illustrated in Fig. 2(c), where the fraction of disorder configurations for the three possible Chern values, $C = 0, 1, 2$, is shown for a specific point in the phase diagram [blue star in Fig. 2(a)] as a function of the disorder strength W . There is an optimal disorder for the $C = 1$ fraction to dominate and the average Chern number to approach $C = 1$ (see the inset). In the thermodynamic limit, it is expected that a finite region with $C = 1$ will develop around the optimal value of disorder. As expected, for higher disorder the system is in a trivial phase. However, a trivial phase also shows up at small disorder, when only one of the ordered phases is established. We conjecture that the rather inhomogeneous CDW induced by disorder in the $C = 1$ phase, as exemplified in Fig. 4, may be the missing ingredient to stabilize the coexistence of the SDW and CDW absent in the clean limit. Nevertheless, the fact that the $C = 1$ phase appears only for high values of disorder indicates that it is a nonperturbative phase and that explanations based on perturbations around the clean limit have to be taken with caution.

Our results manifest the importance of disorder in the boundary regions close to phase transitions. We analyzed the effect of the various parameters (U, V, W) on the boundaries between the $C = 2$ phase and the CDW and SDW in Fig. 2(a) for the $\Delta = 0$ case. We see that Anderson topological insulating phases with $C = 2$ can emerge beyond the phase transition

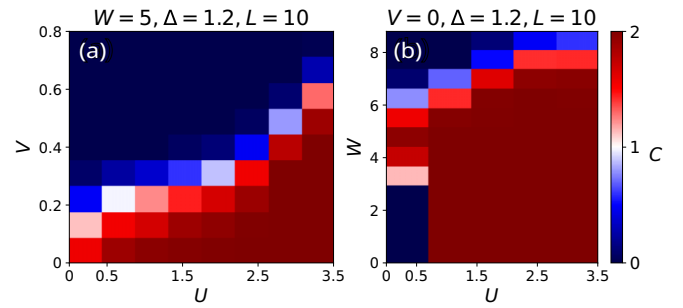


FIG. 6. Phase diagram (a) as a function of U and V for fixed W and (b) as a function of U and W for fixed V for a finite $\Delta = 1.2$. The color map represents the value of the average Chern number. These plots were obtained for a system with linear size $L = 10$ and averaged over 100 disorder configurations. The hopping parameters are the same as the ones used in previous results.

lines of the clean model, as shown in Fig. 2(a), in regions which were previously (for $W = 0$) topologically trivial. Over a critical (interaction dependent) value of disorder, topology disappears, and only trivial insulators remain. Full phase diagrams for different sets of the parameters (U, V, W) can be found in Appendix B.

B. Disorder in the finite- Δ phase diagram.

As mentioned before, an $SU(2)$ broken $C = 1$ phase was previously found in the clean Haldane-Hubbard model as a result of a competition of the SDW insulator driven by U and the trivial insulator driven by the staggered potential Δ [20–23,26,27,29,30]. We analyzed the influence of disorder and the interaction V on that competition for a fixed value of $\Delta = 1.2$. In Fig. 6(a) we show the (U, V) phase diagram for $W = 5$. It can be seen that a $C = 1$ phase appears [white pixel in Fig. 6(a)] at much lower values of U and V . The phase diagram in the (U, W) plane is shown in Fig. 6(b) for $V = 0$. For small values of U , where the clean limit shows trivial behavior, we see a reentrant topological Anderson insulator phase with $C = 2$ as disorder increases. In this context it is worth noting the result discussed in [22], where it was seen that an explicit breakdown of $SU(2)$ from having different hopping amplitudes in the two sublattices led to the $C = 1$ phase even at $U = 0$.

It is worth noting that plateau transitions $C = 2 \rightarrow 1 \rightarrow 0$ are possible with increasing disorder at finite Δ and interactions. Plateau transitions $C = \pm 2 \rightarrow \pm 1 \rightarrow 0$ with increasing disorder are conjectured to be ruled out in quantum Hall systems [31] and other Chern insulators derived from Dirac Hamiltonians [32]. In those systems, starting with $|C| \geq 2$, a plateaus transition $\Delta C = \pm 1$ is never observed with increasing disorder due to ensemble averaging over disorder realizations. Our results for finite disorder in the presence of interactions show that such a transition is possible, in particular if a finite trivial mass is also present.

V. OPEN QUESTIONS AND FUTURE

As mentioned in Sec. III B, an important open question is to make sure that the $C = 1$ phase is not an artifact of the mean-field approximation [27] or a finite-size effect [7]. Ex-

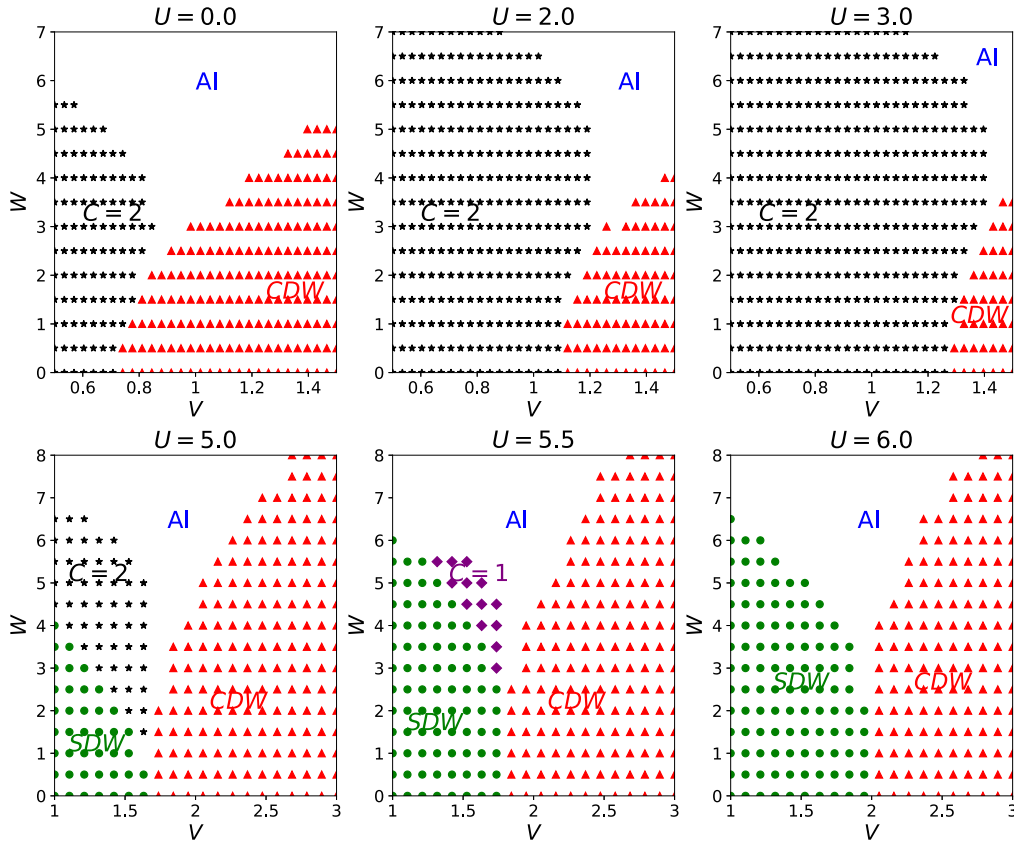


FIG. 7. Phase diagrams as a function of V and W for different choices of U obtained for a system with linear size $L = 10$ and averaged over 50 disorder configurations. The hopping parameters are the same as the ones used in the results presented in the main text.

ploring this region of the parameters with alternative methods like those in [26] would be very enlightening.

Topological phase transitions between $C = 1$ and $C = 0$ or $C = 2$ were found to be of third order in the clean system [20,33]. Disorder makes the analysis of the nature of the phase transitions a hard problem that was left aside in this work, but studying the nature of the phase transition between the $C = 1$ and surrounding phases is worth tackling in the future. This is the problem of the phase transition between a standard insulator and a topological Anderson insulator [34], which is also related to the issue of localization in quantum Hall systems [32,35–37]. Another interesting issue to explore is the structure of the topological edge states in the new phase and their evolution with increasing disorder.

ACKNOWLEDGMENTS

J.S.S. and E.C. acknowledge financial support from FCT-Portugal through Grant No. UIDB/04650/2020. R.M. acknowledges support from NSFC Grants No. NSAF-U2230402, No. 12111530010, No. 12222401, and No. 11974039. M.P.L.-S., M.A.H.V., and J.S.S. acknowledge the support of the Spanish Comunidad de Madrid Grant No. S2018/NMT-4511 (NMT2D-CM). M.A.H.V. is also supported by Spanish Ministerio de Ciencia e Innovación Grant No. PID2021-127240NB-I00. This work was completed during a visit by M.A.H.V. to the Donostia International Physics Center (DIPC), whose kind support is deeply appreciated.

APPENDIX A: MEAN-FIELD CALCULATIONS

In the main text, we described the general methodology to extract the phase diagram of the model. Here, we introduce further technical details. In particular, the procedure to compute the mean-field parameters $\langle c_{i,\sigma}^\dagger c_{j,\sigma'} \rangle$ is as follows: We initialize the parameters (or, in other words, we choose an initial condition for the system); we then diagonalize the Hamiltonian and obtain its eigenvectors and energy spectrum and recalculate the mean-field parameters,

$$\langle c_{i,\sigma}^\dagger c_{j,\sigma'} \rangle = \sum_{E < E_F} [\psi_i^\sigma(E)]^* \psi_j^{\sigma'}(E), \quad (\text{A1})$$

with E_F being the Fermi energy and $\psi_i^\sigma(E)$ being the wave function amplitudes. Finally, we define a convergence threshold ε and repeat the previous steps until $|\langle c_{i,\sigma}^\dagger c_{j,\sigma'} \rangle_{I+1} - \langle c_{i,\sigma}^\dagger c_{j,\sigma'} \rangle_I| < \varepsilon$, with I being the iteration number.

Since a mean-field method can be biased (i.e., the mean-field parameters reached after convergence can be heavily dependent on the choice of initial conditions), we employ a set of initial conditions, apply this procedure to each of them, and choose the solution that yields the lowest ground-state energy for this system (which can be calculated as the sum of the energies of the occupied eigenstates). The simple test of convergence we presented can, in some cases, prove to be very slow to reach convergence. There are many ways of circumventing this issue; we chose to, after each iteration, define the new mean-field parameters as the average of the previous two iterations.

- [1] R. Moessner and J. E. Moore, *Topological Phases of Matter* (Cambridge University Press, Cambridge, 2021).
- [2] S. Rachel, Interacting topological insulators: A review, *Rep. Prog. Phys.* **81**, 116501 (2018).
- [3] P. W. Anderson, Absence of diffusion in certain random lattices, *Phys. Rev.* **109**, 1492 (1958).
- [4] J. Li, R.-L. Chu, J. K. Jain, and S.-Q. Shen, Topological Anderson insulator, *Phys. Rev. Lett.* **102**, 136806 (2009).
- [5] F. D. M. Haldane, Model for a quantum Hall effect without Landau levels: Condensed-matter realization of the “parity anomaly,” *Phys. Rev. Lett.* **61**, 2015 (1988).
- [6] M. Gonçalves, P. Ribeiro, and E. V. Castro, The Haldane model under quenched disorder, [arXiv:1807.11247](https://arxiv.org/abs/1807.11247).
- [7] C. Shao, E. V. Castro, S. Hu, and R. Mondaini, Interplay of local order and topology in the extended Haldane-Hubbard model, *Phys. Rev. B* **103**, 035125 (2021).
- [8] G. Jotzu, M. Messer, R. Desbuquois, M. Lebrat, T. Uehlinger, D. Greif, and T. Esslinger, Experimental realization of the topological Haldane model with ultracold fermions, *Nature (London)* **515**, 237 (2014).
- [9] W. Zhao, K. Kang, L. Li, C. Tschirhart, E. Redekop, K. Watanabe, T. Taniguchi, A. Young, J. Shan, and K. F. Mak, Realization of the Haldane Chern insulator in a moiré lattice, *Nat. Phys.* **20**, 275 (2024).
- [10] M. Greiner, O. Mandel, T. Esslinger, T. W. Hänsch, and I. Bloch, Quantum phase transition from a superfluid to a Mott insulator in a gas of ultracold atoms, *Nature (London)* **415**, 39 (2002).
- [11] T. Esslinger, Fermi-Hubbard physics with atoms in an optical lattice, *Annu. Rev. Condens. Matter Phys.* **1**, 129 (2010).
- [12] A. Rubio-García and J. J. García-Ripoll, Topological phases in the Haldane model with spin-spin on-site interactions, *New J. Phys.* **20**, 043033 (2018).
- [13] E. Guardado-Sanchez, B. M. Spar, P. Schauss, R. Belyansky, J. T. Young, P. Bienias, A. V. Gorshkov, T. Iadecola, and W. S. Bakr, Quench dynamics of a Fermi gas with strong nonlocal interactions, *Phys. Rev. X* **11**, 021036 (2021).
- [14] M. Schreiber, S. S. Hodgman, P. Bordia, H. P. Lüschen, M. H. Fischer, R. Vosk, E. Altman, U. Schneider, and I. Bloch, Observation of many-body localization of interacting fermions in a quasirandom optical lattice, *Science* **349**, 842 (2015).
- [15] J.-Y. Choi, S. Hild, J. Zeiher, P. Schauß, A. Rubio-Abadal, T. Yefsah, V. Khemani, D. A. Huse, I. Bloch, and C. Gross, Exploring the many-body localization transition in two dimensions, *Science* **352**, 1547 (2016).
- [16] S. Sorella and E. Tosatti, Semi-metal-insulator transition of the Hubbard model in the honeycomb lattice, *Europhys. Lett.* **19**, 699 (1992).
- [17] Z. Y. Meng, T. C. Lang, S. Wessel, F. F. Assaad, and A. Muramatsu, Quantum spin-liquid emerging in two-dimensional correlated Dirac fermions, *Nature (London)* **464**, 847 (2010).
- [18] S. Sorella, Y. Otsuka, and S. Yunoki, Absence of a spin liquid phase in the Hubbard model on the honeycomb lattice, *Sci. Rep.* **2**, 992 (2012).
- [19] F. F. Assaad and I. F. Herbut, Pinning the order: The nature of quantum criticality in the Hubbard model on honeycomb lattice, *Phys. Rev. X* **3**, 031010 (2013).
- [20] J. He, Y.-H. Zong, S.-P. Kou, Y. Liang, and S. Feng, Topological spin density waves in the Hubbard model on a honeycomb lattice, *Phys. Rev. B* **84**, 035127 (2011).
- [21] J. He, Y. Liang, and S.-P. Kou, Composite spin liquid in a correlated topological insulator: Spin liquid without spin-charge separation, *Phys. Rev. B* **85**, 205107 (2012).
- [22] T. I. Vanhala, T. Siro, L. Liang, M. Troyer, A. Harju, and P. Törmä, Topological phase transitions in the repulsively interacting Haldane-Hubbard model, *Phys. Rev. Lett.* **116**, 225305 (2016).
- [23] Y.-X. Wang and D.-X. Qi, Spontaneous symmetry breaking of an interacting Chern insulator on a topological square lattice, *Phys. Rev. B* **99**, 075204 (2019).
- [24] T. Mertz, K. Zantout, and R. Valentí, Statistical analysis of the Chern number in the interacting Haldane-Hubbard model, *Phys. Rev. B* **100**, 125111 (2019).
- [25] I. S. Tupitsyn and N. V. Prokof'ev, Phase diagram topology of the Haldane-Hubbard-Coulomb model, *Phys. Rev. B* **99**, 121113(R) (2019).
- [26] H. Yuan, Y. Guo, R. Lu, H. Lu, and C. Shao, Phase transitions in the Haldane-Hubbard model with ionic potentials, *Phys. Rev. B* **107**, 075150 (2023).
- [27] J. Imriška, L. Wang, and M. Troyer, First-order topological phase transition of the Haldane-Hubbard model, *Phys. Rev. B* **94**, 035109 (2016).
- [28] T.-C. Yi, S. Hu, E. V. Castro, and R. Mondaini, Interplay of interactions, disorder, and topology in the Haldane-Hubbard model, *Phys. Rev. B* **104**, 195117 (2021).
- [29] Y.-X. Zhu, J. He, C.-L. Zang, Y. Liang, and S.-P. Kou, Magnetic topological insulators at finite temperature, *J. Phys.: Condens. Matter* **26**, 175601 (2014).
- [30] Y.-J. Wu, N. Li, and S.-P. Kou, Chiral topological superfluids in the attractive Haldane-Hubbard model with opposite Zeeman energy at two sublattice sites, *Eur. Phys. J. B* **88**, 255 (2015).
- [31] Y. Hatsugai, K. Ishibashi, and Y. Morita, Sum rule of Hall conductance in a random quantum phase transition, *Phys. Rev. Lett.* **83**, 2246 (1999).
- [32] Z.-G. Song, Y.-Y. Zhang, J.-T. Song, and S.-S. Li, Route towards localization for quantum anomalous Hall systems with Chern number 2, *Sci. Rep.* **6**, 19018 (2016).
- [33] Y. Shi, Q. Li, J. Yu, J. He, and Y.-J. Wu, Competition between spin density wave and charge density wave driven by interactions of spinful Haldane model on honeycomb lattices, *J. Phys.: Condens. Matter* **33**, 395602 (2021).
- [34] J. T. Chalker, Anderson localisation in quantum Hall systems, *J. Phys. C* **20**, L493 (1987).
- [35] A. W. W. Ludwig, M. P. A. Fisher, R. Shankar, and G. Grinstein, Integer quantum Hall transition: An alternative approach and exact results, *Phys. Rev. B* **50**, 7526 (1994).
- [36] M. Onoda, Y. Avishai, and N. Nagaosa, Localization in a quantum spin Hall system, *Phys. Rev. Lett.* **98**, 076802 (2007).
- [37] R. Shindou and S. Murakami, Effects of disorder in three-dimensional Z_2 quantum spin Hall systems, *Phys. Rev. B* **79**, 045321 (2009).
- [38] T. Fukui, Y. Hatsugai, and H. Suzuki, Chern numbers in discretized Brillouin zone: Efficient method of computing (spin) Hall conductances, *J. Phys. Soc. Jpn.* **74**, 1674 (2005).
- [39] Y.-F. Zhang, Y.-Y. Yang, Y. Ju, L. Sheng, R. Shen, D.-N. Sheng, and D.-Y. Xing, Coupling-matrix approach to the Chern number calculation in disordered systems, *Chin. Phys. B* **22**, 117312 (2013).